ARTICLE NO. 78-1280R

Optimal Open-Loop Maneuver Profiles for Flexible Spacecraft

R. L. Farrenkopf*
TRW Defense and Space Systems Group, Redondo Beach, Calif.

Using the Calculus of Variations, optimal slewing profiles minimizing a structural excitation criterion are established for a dynamically simple spacecraft maneuvering between two quiescent states. Two problem types are considered. In the free-endpoint problem, the structural deformation and its time derivative are unconstrained at maneuver's end. For the constrained-endpoint problem, these variables are required to vanish, which necessarily degrades the excitation criterion. Several figures are presented that illustrate both the nature and the limitations inherent in maneuvering the spacecraft from one attitude state to another. For a given maneuver amplitude $\theta°$, the key parameter influencing structural excitation is the product of the maneuver time T_a and the lowest significant structural frequency ω. It is shown that when $\omega T_a < 5$, a severe excitation penalty results from constraining the terminal structural deformation and its time derivative. When $\omega T_a > 10$, however, this penalty is fairly minor, and some reasonable control of terminal conditions is then practical. Thus it is generally desirable that all maneuver times meet this criterion. When this is the case, it is possible to derive a normalized suboptimal slewing profile $F(x)$ applicable to all maneuvers. Given $\theta°$ and T_a, the commanded maneuver rate becomes $\dot{\theta}(t) = \theta° F(t/T_a)/T_a$. Only a minor computational and memory burden is therefore necessary to perform almost optimal reorientations.

Introduction

MANY spacecraft applications involve maneuvering the vehicle between two quiescent attitude states. If the spacecraft is flexible, significant structural deformation may result when both the maneuver angle is large and the allowed maneuver time short. But these are not the only factors influencing the structural excitation, as the nature of the spacecraft's attitude profile between its two endpoints also plays a critical role. This paper focuses upon establishing maneuver profiles that minimize this excitation, given that a certain maneuver amplitude $\theta°$ must be accomplished within a certain time T_a. Using the Calculus of Variations, an optimal profile is analytically established for a spacecraft characterized by a single significant structural bending mode. The application of this result to more complex structures is then considered.

The term "optimal profile" will be interpreted to mean the extremal solution of a specified quadratic cost criterion (detailed in the next section) involving the structural deformation and its time derivatives. No constraints or cost are associated with the control effort required to effect the maneuver, as is commonly the practice in treating optimal control problems with quadratic criteria. By selecting a particular cost function, a singular control can, nevertheless, be avoided, resulting in a spacecraft maneuver profile with continuous derivatives. The required control function then possesses similar properties on the maneuver interval.

In some applications, the structural deformation during the maneuver is of little importance (as long as excessive stressing does not occur), whereas the deformation and rate at the terminal attitude must necessarily be small. Typical of this case is when a scientific payload mounted on a flexible appendage begins taking data at maneuver's end. In other applications, the reverse situation may exist. Scientific data is taken only during the maneuver, so that terminal structural deformation is of much less importance. This study treats both limiting cases: one where the criterion imposes no constraints on the deformation endpoint (free-endpoint problem), and one where the deformation and its rate are constrained to vanish (constrained endpoint). It is shown that the desire to minimize structural excitation, and the desire to constrain the endpoint deformation are conflicting criteria, in general.

This study was motivated by the results of Ref. 1, which indicated that unless the product of the maneuver time with the lowest significant structural frequency was quite low, it was advantageous to adopt slewing policies with as many continuous time derivatives as possible, i.e., analytic profiles seemed desirable. This leads naturally to the question of what analytic slewing profile excites the spacecraft least, a problem within the realm of the Calculus of Variations. Closed-form solutions are possible because a rather simple, yet practical, dynamic model can be used.

Problem Statement

The following example will be treated in what follows, namely a spacecraft with one flexible appendage containing a single mode of frequency ω. Considerable insight results from the treatment of this simple case, and as mentioned, some degree of generalization is possible.

System Definition

Figure 1 illustrates the system to be analyzed. At time $t = 0$, the following initial conditions are assumed:

$$\theta_a(0) = \dot{\theta}_a(0) = \psi_a(0) = \dot{\psi}_a(0) = 0 \tag{1}$$

and it is required to slew the main body during the time interval $0 \le t \le T_a$ such that

$$\dot{\theta}_a(T_a) = 0 \tag{2}$$

$$\theta(T_a) = \theta° \tag{3}$$

This slewing maneuver is to be performed in such a way that the modal excitation (involving the derivatives of ψ_a) is

Presented as Paper 78-1280 at the AIAA Guidance and Control Conference, Palo Alto, Calif., Aug. 7-9, 1978; submitted Sept. 1, 1978; revision received Feb. 1, 1979.

Index category: Spacecraft Dynamics and Control.

*Senior Staff Engineer, Systems Engineering. Member AIAA.

minimized over the time interval $[0, T_a]$ while satisfying any endpoint constraints, if specified.

The equations of motion describing the system of Fig. 1 are given by

$$\ddot{\psi}_a + \omega^2 \psi_a = -\ddot{\theta}_a \tag{4}$$

$$\ddot{\theta}_a - \eta\omega^2 \psi_a = u \tag{5}$$

where η is the ratio of appendage to main body moment of inertia, and u is the control torque to main body moment of inertia. The optimal scan profiles can be derived solely from Eq. (4), so no further use will be made of Eq. (5) in this paper. The latter is useful only to derive the necessary control effort u, once the θ_a and ψ_a profiles have been derived.

Normalizing the System Parameters

It becomes convenient, in what follows, to normalize the system variables. Define

$$T = \omega T_a \tag{6}$$

$$\theta(\omega t) = \theta_a(t)/\theta^\circ \qquad \psi(\omega t) = \psi_a(t)/\theta^\circ \tag{7}$$

Then

$$\left.\begin{aligned} \dot{\psi} &= \frac{1}{\omega}\left(\frac{\dot{\psi}_a}{\theta^\circ}\right) & \dot{\theta} &= \frac{1}{\omega}\left(\frac{\dot{\theta}_a}{\theta^\circ}\right) \\ \ddot{\psi} &= \frac{1}{\omega^2}\left(\frac{\ddot{\psi}_a}{\theta^\circ}\right) & \ddot{\theta} &= \frac{1}{\omega^2}\left(\frac{\ddot{\theta}_a}{\theta^\circ}\right) \end{aligned}\right\} \tag{8}$$

and Eq. (4) reduces to

$$\ddot{\psi} + \psi = -\ddot{\theta} \tag{9}$$

with the boundary conditions

$$\psi(0) = \dot{\psi}(0) = \theta(0) = \dot{\theta}(0) = 0 \tag{10}$$

$$\dot{\theta}(T) = 0 \tag{11}$$

$$\theta(T) = 1 \tag{12}$$

Criterion Selection

A meaninfgul endpoint criterion is to measure the extent to which the bending mode must damp out for $t > T_a$. One such measure is, in normal form, given by the *residual*

$$R = \sqrt{\psi^2(T) + \dot{\psi}^2(T)} \tag{13}$$

The importance of R depends on the mission, as was mentioned.

The criterion for measuring the structural excitation during the maneuver will be taken as

$$E = \left[\frac{1}{T}\int_0^T (\dot{\psi}^2 + \ddot{\psi}^2)\, dt\right]^{1/2} \tag{14}$$

This is not the most preferable excitation criterion in the author's view. An intuitively better selection for the integrand in Eq. (14) might be the instantaneous structural energy $\psi^2 + \dot{\psi}^2$. The energy integrand, unfortunately, does not yield an extremal solution for the constrained-endpoint problem implying, instead, a singular control as optimal. A nonsingular optimal control is possible for the latter case if the excitation criterion is altered to include a quadratic loss term involving control effort, but at significant increase in analytic complexity. To keep things simple, the author chose to take Eq. (14) as his excitation criterion, as this yields extremal solutions for both the free- and constrained-endpoint problems. Qualitative justification for the integrand of this equation might be based upon the fact that, when normalized, $\ddot{\psi}^2 = \psi^2$ for a sinusoidally vibrating appendage, but a better defense is provided by the intuitively reasonable results that this criterion offers, as will be seen shortly.

The above criteria are now combined in the single cost function for which a minimum is sought:

$$J = A'R + E \tag{15}$$

where A' is some predetermined constant which weights R against E. $\theta(t)$ will be established on the interval $[0, T]$ to minimize J. Note that when A' is chosen very small, a free-endpoint problem results. Very large A' will yield solutions to the constrained-endpoint problem.

Solution for the Extremal (Optimal) $\theta(t)$ on $[0, T]$

The optimal slew profiles are derived in the Appendix. Denoting the optimal $[\theta(t), \psi(t)]$ profile by $[\theta_0(t), \psi_0(t)]$, it turns out that

$$\begin{aligned} \theta_0(t) = {} & \alpha_0(2 + t^2/2 - 2\cosh t) \\ & + k_1(4t + 2t^3/3 + t^5/60 - 4\sinh t) \\ & + k_2(2 + t^2 + t^4/24 - 2\cosh t) \\ & + k_3(2t + t^3/6 - 2\sinh t) \end{aligned} \tag{16}$$

$$\begin{aligned} \psi_0(t) = {} & \alpha_0(\cosh t - 1) \\ & + k_1(2\sinh t - 2t - t^3/3) \\ & + k_2(\cosh t - 1 - t^2/2) \\ & + k_3(\sinh t - t) \end{aligned} \tag{17}$$

where α_0, k_1, k_2, and k_3 are constants whose values are fixed by the boundary conditions. Their evaluation follows from

$$[\alpha_0 k_1 k_2 k_3]^t = A_0^{-1}[0 -1\ 0\ 0]^t \tag{18}$$

where the superscript t denotes matrix transpose and where A_0 is a matrix whose components are

$$\begin{aligned} a_{11} &= 2S_T - T & a_{12} &= 4(C_T - 1) - 2T^2 - \frac{T^4}{12} \\ a_{13} &= 2(S_T - T) - \frac{T^3}{6} & a_{14} &= 2(C_T - 1) - \frac{T^2}{2} \\ a_{21} &= 2(C_T - 1) - \frac{T^2}{2} & a_{22} &= 4(S_T - T) - \frac{2T^3}{3} - \frac{T^5}{60} \\ a_{23} &= 2(C_T - 1) - T^2 - \frac{T^4}{24} & a_{24} &= 2(S_T - T) - \frac{T^3}{6} \\ a_{31} &= C_T - 1 & a_{32} &= 2(S_T - T) - \frac{T^3}{3} \\ & & & \quad - \frac{1}{A}(T^2 - 2) \\ a_{33} &= C_T - 1 - \frac{T^2}{2} - \frac{T}{A} & a_{34} &= S_T - T - \frac{1}{A} \\ a_{41} &= C_T + AS_T & a_{42} &= 2S_T - 4T \\ & & & \quad + A(2C_T - T^2 - 2) \\ a_{43} &= C_T - 2 + A(S_T - T) & a_{44} &= S_T + A(C_T - 1) \end{aligned} \tag{19}$$

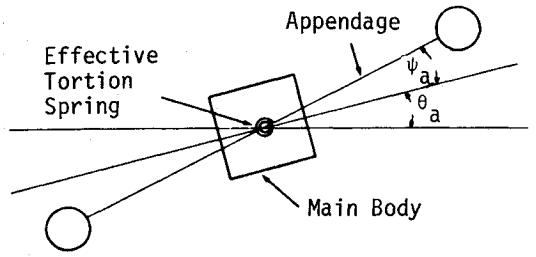

Fig. 1 Schematic of system to be analyzed.

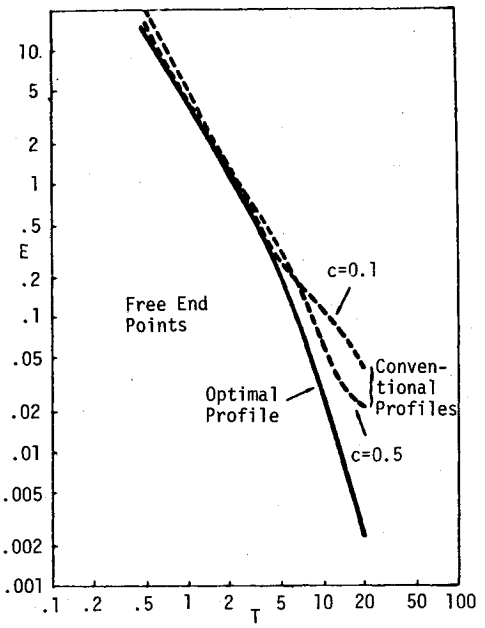

Fig. 2 Excitation vs normalized maneuver time.

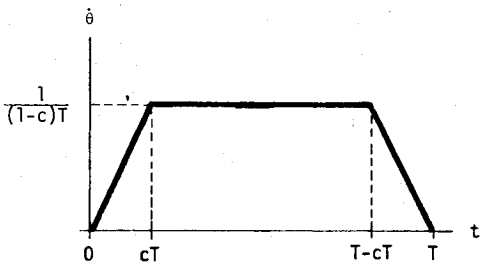

Fig. 3 Conventional control profiles.

where

$$S_T = \sinh T \qquad C_T = \cosh T \tag{20}$$

and A is proportional to the preselected constant A', described above.

As mentioned before, knowledge of $\theta_0(t)$ and $\psi_0(t)$ permits calculation of the optimal control function by first converting these normalized functions back to their actual counterparts, and then using Eq. (5).

Results and Conclusions

Free-Endpoint Problem

Figure 2 presents the minimal extremal excitation E as a function of its dominant parameter T. For comparison purposes, two "conventional" control results are also plotted, in which the $\dot\theta(t)$ profile is indicated by Fig. 3. Note that the latter do not meet the smoothness characteristics associated with the optimal profile in that their second derivatives with respect to time are not everywhere continuous.

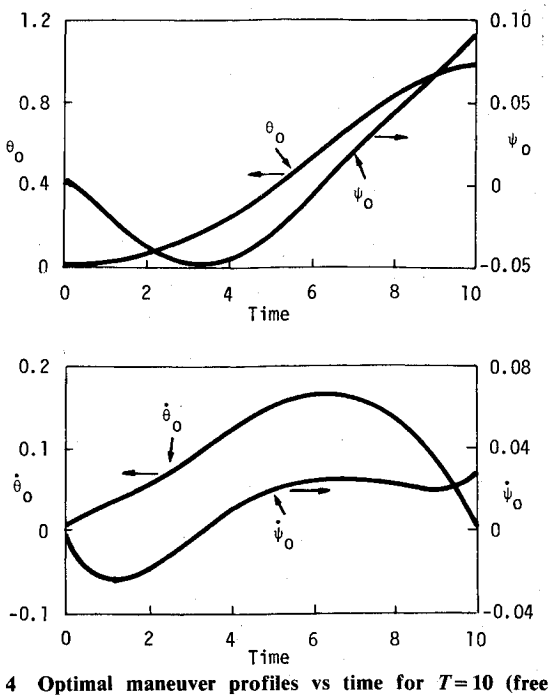

Fig. 4 Optimal maneuver profiles vs time for $T=10$ (free endpoints).

Figure 2 indicates little difference among the three profiles for $T<5$, and large excitations result in this region. This is because the flexible mode is just too "soft" when compared to the response time demanded of the spacecraft main body. For $T>5$, the optimal profile dominates its conventional rivals by more and more, so that at $T=20$ an order of magnitude improvement is realized.

An example for $T=10$ is shown in Fig. 4. θ_0 and $\dot\theta_0$ meet their required boundary conditions, and it is interesting to compare the optimal $\dot\theta$ profile to the conventional profiles of Fig. 3. Note that for $T=10$ the residual is quite small even though this is a free-endpoint problem.

A comparable example for $T=1$ is shown in Fig. 5. The relative softness of the flexible mode yields large terminal values for ψ and $\dot\psi$, i.e., a large residual.

Constrained-Endpoint Problem

Recall that here it is required that $\psi_0(T) = \dot\psi_0(T) = 0$. Figure 6 illustrates the tradeoff between E and R obtained as A' in Eq. (15) ranges from very small to very large values. Consider first the $T=10$ curve. Here the residual is quite small even for free endpoints, and there is little penalty in causing R to vanish. One would expect the $\dot\theta_0(t)$ profiles for these extremes in A' to be reasonably similar.

At the other end of the scale, when $T=0.5$, there are several orders of magnitude increase in E in going from free to constrained ends. Most of this increase takes place without a comparable reduction in R, i.e., drastic measures are required to cause any change in the free positions of $\psi_0(T)$ and $\dot\psi_0(T)$. The $\dot\theta_0(t)$ profiles for free and constrained ends will thus differ widely.

Figure 7 is an example of a constrained optimal profile for $T=10$. As required, $\psi_0(T) = \dot\psi_0(T) = 0$. Note also the symmetric nature of both $\dot\theta_0$ and $\dot\psi_0$.

Figure 8 is a similar example for $T=1$. Although the required terminal conditions are met, note the violent nature of the response on the interval [0, 1]. Although θ_0 is required only to terminate at unity, it reaches magnitudes in excess of 7 in order to "pin" the terminal values of ψ_0 and its derivative. The large increase in excitation thus accompanies this behavior.

Often a particular bending mode frequency may be imprecisely known, and it is desirable to determine the impact on

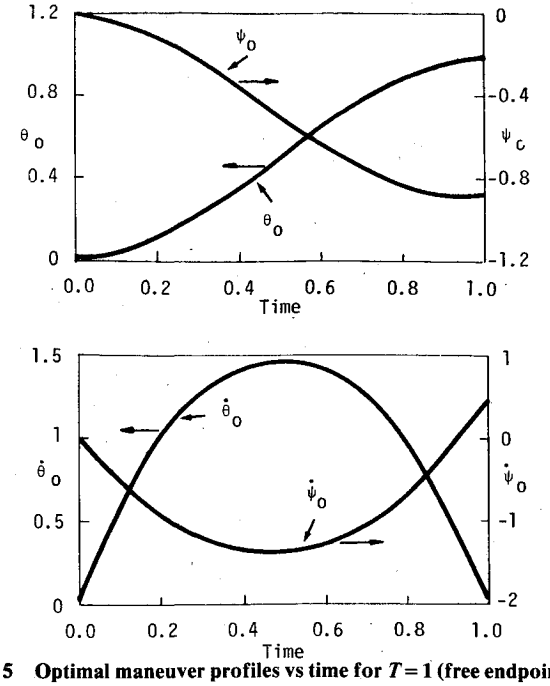

Fig. 5 Optimal maneuver profiles vs time for $T=1$ (free endpoints).

such a mode of an optimal profile based upon a somewhat different estimate. For a profile based on a frequency $\omega_{nom}=1$, Fig. 9 illustrates E and R when the actual bending mode frequency is actually ω for the case where $T=\omega_{nom}T_a=10$. It is seen that E is monotonically decreasing for $\omega>\omega_{nom}$, although decreasing at a slower rate than if the optimal profile for ω had been used. For $\omega<\omega_{nom}$, there is little difference between the optimal possible E and that caused by the ω_{nom} profile.

Some penalty in the residual results from driving modes for which $\omega/\omega_{nom}\neq 1$ with the optimal profile for ω_{nom}. Had such modes been driven by their own optimals, their residuals would have vanished. Figure 9 indicates that driving higher frequency modes by the ω_{nom} profile results in a normalized residual of 0.05 or less. If this is acceptable, the simple model assumed still provides an effective means for generating optimal profiles.

Figure 10 similarly checks the effect on other modes when $T=1$. The previous conclusions regarding excitation still hold† but the violent nature of $\dot\theta_0(t)$ for ω_{nom} raises havoc with the residuals of modes that depart very much from this frequency. One concludes that for small values of T, constraining the endpoints of a multiflexible mode spacecraft appendage, while not mathematically impossible, is certainly impractical.

A Normalized Constrained-Endpoint Maneuver Profile

If the lowest significant spacecraft structural mode has frequency ω, and T_a represents the minimum slew time between two quiescent main body attitudes, Fig. 6 indicates that little penalty is incurred by constraining the endpoint ($R=0$) if $T=\omega T_a>10$. In many applications this condition can be satisfied for all maneuvers, but as different slew times are usually dictated, T may take on many different values exceeding 10, each requiring a separate, rather cumbersome, profile calculation, as previously described. It seemed likely that as T gets larger and larger, the shape of the $\dot\theta_0(t)$ profile would converge, and this indeed happens. Table 1 shows values of $T\dot\theta_0(t/T)$ for values of T ranging from 10 to 30. (Note that $\dot\theta_0$ need only be specified for $0\le t/T\le 0.5$, as this function is symmetric for all T when the endpoints are constrained.)

$$\dot\theta_0(T-t)=\dot\theta_0(t) \tag{21}$$

Clearly the anticipated convergence takes place. Thus rather than calculate a separate $\theta_0(t)$ profile for every ωT_a combination, a significant computational burden can be alleviated by prestoring the normalized form, $F(x)$, of one of the Table 1 trajectories, say the one for $T=20$. Figure 9, discussed before, indicates that, at most, only a minor penalty results. Almost optimal profiles (for $T>10$) are then derived from the $T=20$ profile, which is illustrated in Fig. 11. The commanded rate, $\dot\theta_a(t)$, satisfies

$$\dot\theta_a(t)=(\theta^\circ/T_a)F(t/T_a) \tag{22}$$

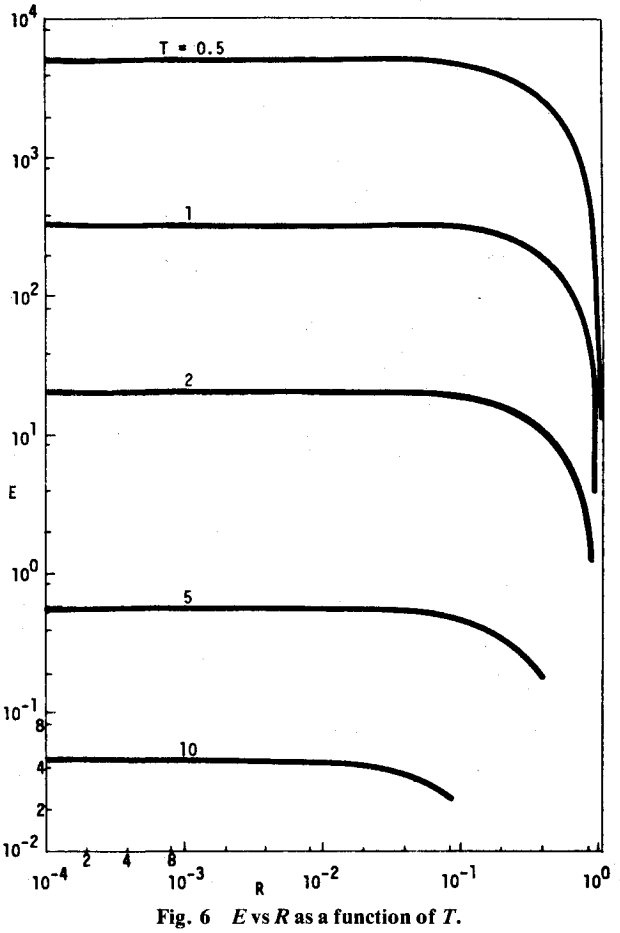

Fig. 6 E vs R as a function of T.

Table 1 Optimal $\dot\theta$ profiles vs T

	$T\dot\theta_0(t/T)$				
$x=t/T$	$T=10$	$T=15$	$T=20$	$T=25$	$T=30$
0	0	0	0	0	0
0.05	0.373	0.195	0.130	0.100	0.081
0.10	0.549	0.326	0.252	0.223	0.207
0.15	0.678	0.494	0.446	0.433	0.423
0.20	0.824	0.720	0.702	0.705	0.702
0.25	0.998	0.986	0.996	1.008	1.002
0.30	1.188	1.259	1.290	1.305	1.299
0.35	1.371	1.509	1.552	1.568	1.557
0.40	1.552	1.709	1.758	1.773	1.761
0.45	1.622	1.838	1.890	1.903	1.890
0.50	1.656	1.881	1.934	1.948	1.935

†Note that when $\omega<\omega_{nom}$, its optimal profile E exceeds that for the ω_{nom} profile. This is because the latter violates the desired endpoint constraints.

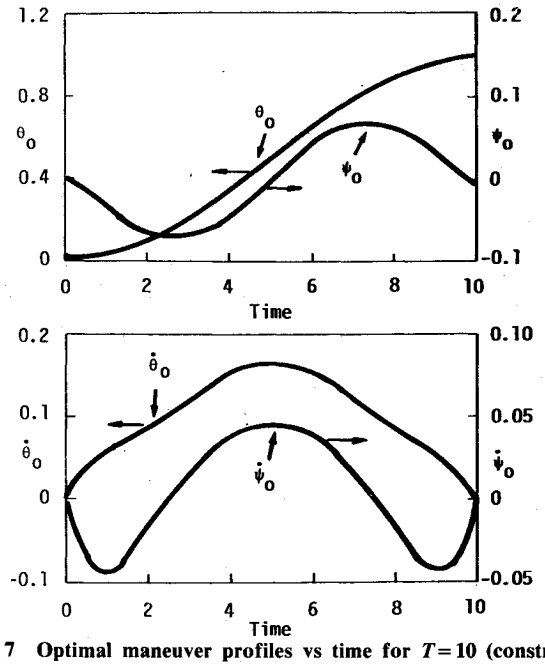

Fig. 7 Optimal maneuver profiles vs time for $T=10$ (constrained endpoints).

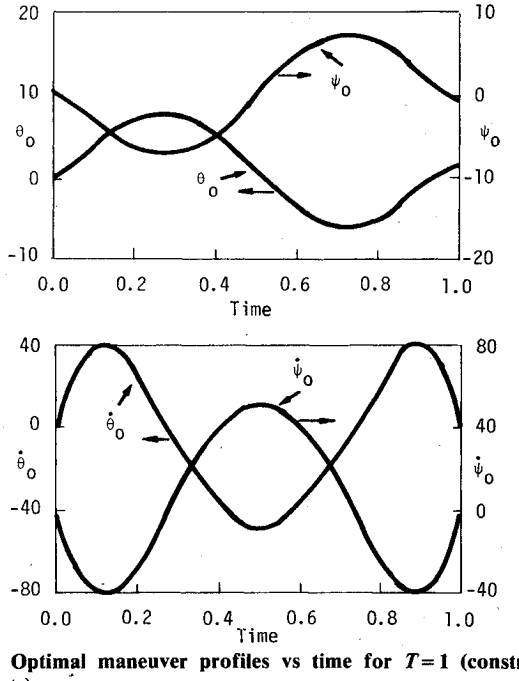

Fig. 8 Optimal maneuver profiles vs time for $T=1$ (constrained endpoints).

where θ° and T_a are, respectively, the actual maneuver amplitude and time, and $F(x)$ is given in Fig. 11.

Generalization to More Complex Spacecraft

Suppose now that we consider a spacecraft with many more than a single structural bending mode. Assuming a finite-element approach, let ψ be an n-dimensional angular structural deformation vector *relative* to the undeformed coordinate axes whose orientation is defined by θ. Assuming small (first-order) orientations and deformations, the system equations of motion have the appearance

$$\begin{bmatrix} M_0 & 0 \\ M_1 & M_2 \end{bmatrix} \begin{bmatrix} \ddot{\theta} \\ \ddot{\psi} \end{bmatrix} + \begin{bmatrix} 0 & K_1 \\ 0 & K_2 \end{bmatrix} \begin{bmatrix} \theta \\ \psi \end{bmatrix} = \begin{bmatrix} u \\ 0 \end{bmatrix} \tag{23}$$

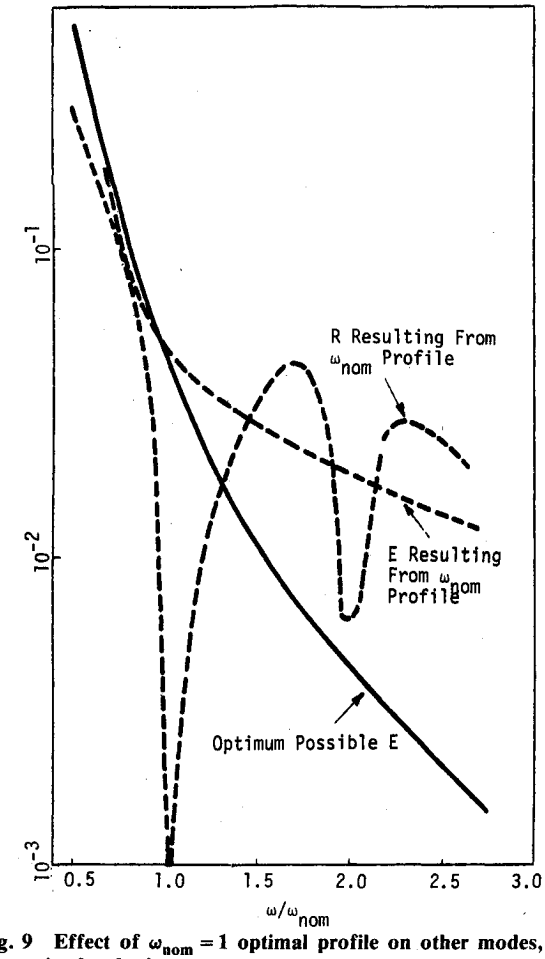

Fig. 9 Effect of $\omega_{nom}=1$ optimal profile on other modes, $T=10$, constrained endpoints.

From Eq. (23), it follows that

$$M_2\ddot{\psi}+K_2\psi=-M_1\ddot{\theta} \tag{24}$$

Premultiplying by M_2^{-1}, and converting to normal coordinates, η, through use of the modal matrix Φ, it follows that

$$\ddot{\eta}+\Lambda\eta=-\Phi^{-1}M_2^{-1}M_1\ddot{\theta} \tag{25}$$

where

$$\psi=\Phi\psi \tag{26}$$

$$\Lambda=\Phi^{-1}M_2^{-1}K_2\Phi=\text{diag}\ (\omega_1^2, \omega_2^2 \ldots \omega_n^2) \tag{27}$$

Equation (25) defines a set of uncoupled scalar differential equations of the same form as Eq. (4), namely

$$\ddot{\eta}_i+\omega_i^2\eta_i=-a_i\ddot{\theta} \qquad (i=1, 2, \ldots n) \tag{28}$$

Given θ°, T_a, and a maneuver profile, $\dot{\theta}(t)$, Eq. (28) defines the response of each system structural mode.

Having derived the system equations, it is now possible to define a quadratic excitation criterion involving each $\dot{\eta}_i$ and $\ddot{\eta}_i$, and to seek the $\dot{\theta}(t)$ profile that minimizes this excitation for either free or constrained terminal conditions on sructural deformation. This is a complex problem beyond the scope of this paper. However, the solution previously obtained for the simple configuration of Fig. 1 has some utility for this multimode problem as well. Noting Eq. (28), the most severely affected modes are those of low frequency for which a_i is significant, for it is for these modes that T assumes its least values. Thus, the optimal maneuver profile should be based on the lowest frequency bending mode for which the

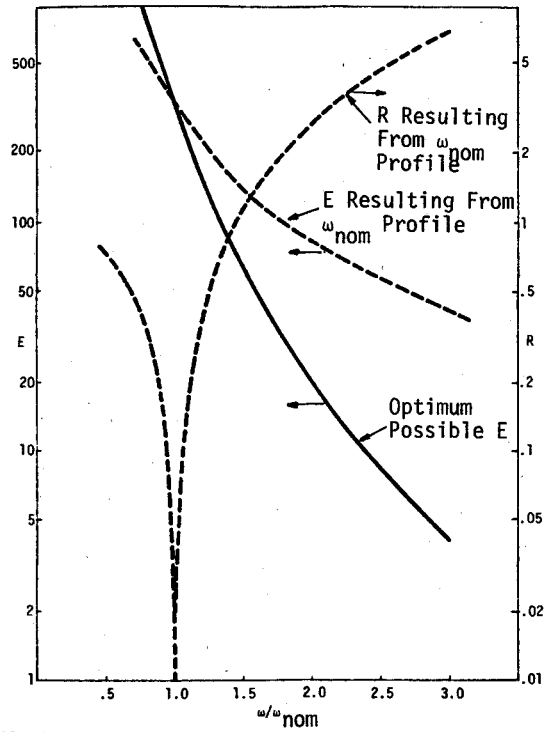

Fig. 10 Effect of ω_{nom} optimal profile on other modes, $T=1$, constrained endpoints.

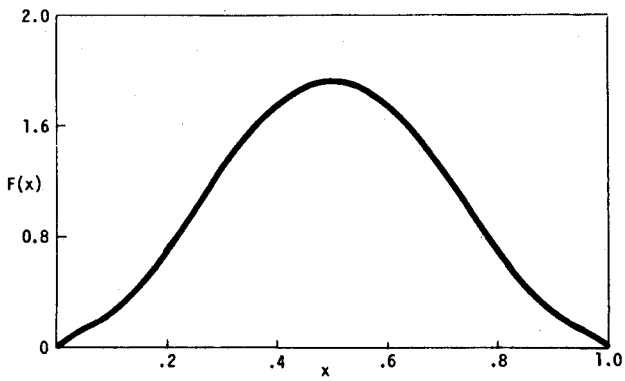

Fig. 11 Normalized suboptimal maneuver profile.

excitation parameter a_i has influence. For similar excitation parameter values, modes higher in frequency display a monotonically decreasing excitation (see Fig. 9), and those lower in frequency are only minimally affected due to their meager a_i. In this way the solution for the simple single-mode example can often be applied to multimode applications as well.

Conclusions

Based on a defined bending mode excitation criterion, optimal slewing profiles have been established for a single structural mode spacecraft maneuvering between two quiescent states. Several important conclusions were then derived. It was shown that the most important parameter affecting structural excitation is the product of the maneuver time T_a and the lowest significant structural frequency ω. When $\omega T_a < 5$, a severe excitation penalty results from constraining the terminal structural deformation and its time derivative. For $\omega T_a > 10$, such constraints have much less influence. For the latter case, a normalized suboptimal slewing profile was presented, applicable to all such maneuvers. Finally, a limited generalization of these results to dynamically more complex spacecraft was demonstrated. It is hoped that the insight gained from consideration of this simple example will prove beneficial in the maneuver design of practical spacecraft.

Appendix

Optimum Maneuver Profiles

Given the system

$$\ddot{\psi}(t)+\psi(t)=-\ddot{\theta}(t)\quad t\epsilon[0,T] \tag{A1}$$

$$\theta(0)=\dot{\theta}(0)=\psi(0)=\dot{\psi}(0)=\dot{\theta}(T)=0 \tag{A2}$$

$$\theta(T)=1 \tag{A3}$$

it is required to establish the optimal maneuver profile, $\theta(t)$, $t\epsilon[0,T]$, that will minimize the criterion

$$J=A'R+E \tag{A4}$$

where A' is some pre-established constant and

$$R=[\psi^2(T)+\dot{\psi}^2(T)]^{1/2} \tag{A5}$$

$$E=\left[\frac{1}{T}\int_0^T F(\dot{\psi},\ddot{\psi})\mathrm{d}t\right]^{1/2} \tag{A6}$$

where

$$F(\dot{\psi},\ddot{\psi})=\dot{\psi}^2+\ddot{\psi}^2 \tag{A7}$$

The subscript 0 will denote conditions for the optimal trajectory. Thus, when $\psi(t)$ is optimal (in that it minimizes J) then $\psi(t)=\psi_0(t)$, $R=R_0$, $E=E_0$, $J=J_0$, etc.

Defining μ and β by the conditions that

$$\dot{\psi}-\mu=0 \tag{A8}$$

$$\dot{\theta}-\beta=0 \tag{A9}$$

Eq. (A1) becomes

$$\dot{\mu}+\psi+\dot{\beta}=0 \tag{A10}$$

Equations (A8-A10) will be termed "side conditions." Integrating Eq. (A1) in light of the initial conditions on ψ and $\dot{\psi}$, it follows that in terms of the new variables, the boundary conditions [Eqs. (A2) and (A3)] are satisfied if

$$\psi(0)=0 \tag{A11}$$

$$\mu(0)=0 \tag{A12}$$

$$\mu(T)+\int_0^T\psi(s)\mathrm{d}s=0 \tag{A13}$$

$$\psi(T)+\int_0^T\left[\int_0^t\psi(s)\mathrm{d}s\right]\mathrm{d}t=-1 \tag{A14}$$

Equations (A5-A7) become, respectively

$$R=[\psi^2(T)+\mu^2(T)]^{1/2} \tag{A15}$$

$$E=\left[\frac{1}{T}\int_0^T F(\mu,\dot{\mu})\mathrm{d}t\right]^{1/2} \tag{A16}$$

$$F(\mu,\dot{\mu})=\mu^2+\dot{\mu}^2 \tag{A17}$$

Necessary conditions for an optimal trajectory can now be derived by using the time-varying Lagrange multipliers $\lambda_i(i=1,2,3)$, and appending the side conditions to J to form

$$G=J+\int_0^T \lambda_1'(\dot{\theta}-\beta)\,dt+\int_0^T \lambda_2'(\dot{\psi}-\mu)\,dt + \int_0^T \lambda_3'(\dot{\mu}+\dot{\beta}+\psi)\,dt \tag{A18}$$

Proceeding in the standard way, we now consider a first-order variation in each of the states ψ, θ, β, μ about its optimal trajectory, and note that for optimality its effect upon G must vanish, i.e.,

$$\delta G=0 \tag{A19}$$

Constraints must be placed on these variations, however, due to the vanishing initial conditions on ψ, μ, θ, and β, i.e. no variation at $t=0$ is permitted. Thus,

$$\delta\theta(0)=\delta\beta(0)=\delta\psi(0)=\delta\mu(0)=0 \tag{A20}$$

θ and its derivative, β, are also fixed at $t=T$, again requiring that

$$\delta\theta(T)=\delta\beta(T)=0 \tag{A21}$$

No specific constraints, however, prevent $\psi(T)$ or $\mu(T)$ from undergoing a small change, so $\delta\psi(T)$ and $\delta\mu(T)$ are, as yet, unconstrained. A formal variation of Eq. (A18) is now taken, imposing Eq. (A19). Multiplying the result by $2E_0T$, it follows that

$$2A\psi_0(T)\delta\psi(T)+2A\mu_0(T)\delta\mu(T) + \int_0^T [F_\mu\delta\mu+F_{\dot\mu}\delta\dot\mu+\lambda_1(\delta\dot\theta-\delta\beta)+\lambda_2(\delta\dot\psi-\delta\mu) +\lambda_3(\delta\dot\mu+\delta\dot\beta+\delta\psi)]\,dt=0 \tag{A22}$$

where

$$\lambda_i=2E_0T\lambda_i' \qquad (i=1,2,3) \tag{A23}$$

$$A=(E_0T/R_0)A' \tag{A24}$$

$$F_\mu=\frac{\partial F}{\partial\mu}(\mu_0,\dot\mu_0) \tag{A25}$$

$$F_{\dot\mu}=\frac{\partial F}{\partial\dot\mu}(\mu_0,\dot\mu_0) \tag{A26}$$

Integrating by parts Eq. (A22) terms involving variational derivatives, and imposing the conditions of Eqs. (A20) and (A21), leads Eq. (A22) to the form

$$\delta G=\int_0^T\left[\left(F_\mu-\frac{d}{dt}F_{\dot\mu}-\lambda_2-\dot\lambda_3\right)\delta\mu + (\lambda_3-\dot\lambda_2)\delta\psi-(\lambda_1+\dot\lambda_3)\delta\beta-\dot\lambda_1\delta\theta\right]dt + [2A\psi_0(T)+\lambda_2(T)]\delta\psi(T) + [F_{\dot\mu}(T)+2A\mu_0(T)+\lambda_3(T)]\delta\mu(T)=0 \tag{A27}$$

Because of the arbitrary nature of $\delta\psi$, $\delta\mu$, $\delta\beta$, and $\delta\theta$, this leads to the Euler necessary conditions

$$\frac{d}{dt}F_{\dot\mu}-F_\mu+\lambda_2+\dot\lambda_3=0 \tag{A28}$$

$$\dot\lambda_2-\lambda_3=0 \tag{A29}$$

$$\dot\lambda_3+\lambda_1=0 \tag{A30}$$

$$\dot\lambda_1=0 \tag{A31}$$

and the transversatility conditions

$$2A\psi_0(T)+\lambda_2(T)=0 \tag{A32}$$

$$F_{\dot\mu}(T)+2A\dot\mu_0(T)+\lambda_3(T)=0 \tag{A33}$$

Equations (A28-A33), subject to the appropriate boundary conditions, will provide the optimal $[\theta_0(t),\ \psi_0(t)]$ that we seek.

Equations (A29-A31) are simply solved to yield

$$\lambda_3=-c_1t+c_2 \tag{A34}$$

$$\lambda_2=-\frac{c_1}{2}t^2+c_2t+c_3 \tag{A35}$$

where the c_i are constants. Now making use of Eq. (A17) in Eq. (A28), it follows that

$$\ddot\mu_0-\mu_0=k_1t^2+k_2t+k_3 \tag{A36}$$

where

$$k_1=c_1/4 \qquad k_2=-c_2/2 \qquad k_3=(c_1-c_3)/2 \tag{A37}$$

The general solution to Eq. (A36) contains two arbitrary constants in addition to k_1, k_2, and k_3. One of these vanishes, however, in order to satisfy Eq. (A12). Thus

$$\mu_0(t)=\alpha_0\sinh t+k_1[-(t^2+2)+2\cosh t] +k_2[-t+\sinh t]+k_3[\cosh t-1] \tag{A38}$$

Integrating this equation yields $\psi_0(t)$, where the constant of integration vanishes to satisfy Eq. (A11). Thus

$$\psi_0(t)=\alpha_0[\cosh t-1]+k_1[2\sinh t-2t-t^3/3] +k_2[\cosh t-1-t^2/2]+k_3[\sinh t-t] \tag{A39}$$

The four constants α_0, k_1, k_2, k_3 are fixed by Eqs. (A13), (A14), (A32), and (A33), once the latter two equations are expressed in terms of the k_i. This is done using Eqs. (A34), (A35), and (A37). Equations (A32) and (A33) then become

$$\psi_0(T)-(1/A)[(T^2-2)k_1+Tk_2+k_3]=0 \tag{A40}$$

$$\dot\mu_0(T)+A\mu_0(T)-2Tk_1-k_2=0 \tag{A41}$$

The first constraint equation follows from Eq. (A13) by integrating Eq. (A39), evaluating it at time T, and adding it to $\mu(T)$, obtained from Eq. (A38). The second constraint equation follows in a similar fashion by applying Eq. (A14). Equation (A40) yields the third constraint equation upon using Eq. (A39) at time T, and Eq. (A41) yields the fourth constraint upon using Eq. (A38) and its time derivative.

The four linear equations can be represented in matrix form as

$$A_0[\alpha_0k_1k_2k_3]^t=[0-1\,0\,0]^t \tag{A42}$$

where the components af A_0 are given by Eq. (19) of this paper's main body.

$\psi_0(t)$ in Eq. (A39) can now be quantified. From Eq. (A1) and its boundary conditions

$$\theta_0(t)=-\psi_0(t)-\int_0^T\left[\int_0^s\psi_0(x)\,dx\right]ds \tag{A43}$$

it follows that

$$\theta_0(t) = \alpha_0(2+t^2/2-2\cosh t) + k_1(4t+2t^3/3+t^5/60-4\sinh t) + k_2(2+t^2+t^4/24-2\cosh t) \quad k_3(2t+t^3/6-2\sinh t) \qquad \text{(A44)}$$

Equations (A39) and (A44) provide a complete solution of this problem.

References

[1] Lassen, H. A. and Elliott, L. E., "Use of Control of Higher Order Derivatives of Excitation to Minimize Dynamic Response," TRW IOC, Jan. 7, 1977.